

# Early Career Materials Researcher Research Letter



# High surface area and dual heteroatom-doped carbon fibers derived from polypropylene masks for CO<sub>2</sub> capture

Alejandro Güillen Obando, Mark Robertson, Paul Smith, Zhe Qiang<sup>®</sup>, School of Polymer Science and Engineering, The University of Southern Mississippi, 118 College Dr, Hattiesburg, MS 39406, USA

Address all correspondence to Zhe Qiang at zhe.qiang@usm.edu

(Received 21 March 2023; accepted 31 July 2023; published online: 7 August 2023)

#### **Abstract**

 ${
m CO_2}$  emission and plastic pollution represent two major, grand-scale, and interconnected environmental challenges. Despite intensive efforts, solutions that can concurrently address both are still in general lacking. Unlock the potential of plastic waste for  ${
m CO_2}$  capture would be ideal toward developing a circular economy and sustainable future. In this work, we demonstrate the use of polypropylene masks as the precursors for fabricating nitrogen and sulfur co-doped carbon fibers with high surface areas. These materials can exhibit an excellent  ${
m CO_2}$  uptake capacity of 4.8 mmol/g at room temperature and 1 bar and a high  ${
m CO_2/N_2}$  selectivity up to 78. This work provides a feasible and scalable approach for upcycling of fibril polyolefin wastes to porous environmental remediation sorbents.

### Introduction

Constant, large-scale greenhouse gas emissions into the atmosphere can lead to adverse environmental and health impacts, such as more severe weather events, sea-level rise, and respiratory diseases<sup>[1,2]</sup>; 37.9 gigaton of CO<sub>2</sub> was emitted into the atmosphere just in 2021. Establishing realistic technology pathways for achieving a carbon–neutral society is of urgent importance for the future of our society and planet. Among various efforts, development of high-performance carbon capture sorbents represents a strong need, which can capture CO<sub>2</sub> directly from flue gas streams and/or air. For example, the use of porous carbons as solid sorbents for CO<sub>2</sub> capture has received significant attention due to their advantages of excellent chemical, thermal, and morphological stability, as well as the compatibility with additional chemistry for pore surface modification/functionalization.<sup>[3-5]</sup>

While there are various routes for preparing porous carbons, using plastic waste as the starting materials is particularly compelling due to its potential to address the need of plastic waste remediation, while producing materials with enhanced value. [6,7] One exciting method in this area is through Flash joule heating, which can readily convert any type of plastic wastes to high-quality graphene materials. [8,9] This technology relies on the application of sequential alternating current and direct current to induce extremely high temperatures in a short time period, breaking down carbon sources and allowing the synthesis of stacked graphene layers without the use of solvent and reactive gases. Alternatively, direct pyrolysis of plastic waste is a commercially viable approach due to its ease in scaling up.[10,11] However, most polymers have a very low carbon yield, and thus a crosslinking step is typically necessary. For polyolefin-based wastes, including polyethene (PE),

polypropylene (PP), and thermoplastic elastomers, sulfonation reaction is an efficient method to crosslink their polymer backbones, enabling them to become carbon precursors. Following pyrolysis at temperatures above 600°C, more than 50 wt% of carbon yields can be achieved.[12,13] In a seminal work, Pol and co-workers reported the synthesis of amorphous carbon chips through pyrolysis-based PE waste upcycling, which can be used as active anode materials in Li-ion battery. [14] Similarly, Yang and co-workers showed that PE-derived mesoporous carbon can enable highly efficient supercapacitors. [15] As demonstrated by these examples, conversion of plastic wastes to carbon materials is a very promising upcycling strategy for achieving enhanced value through addressing energy and environmental applications. Additionally, carbon materials can be used in multiple other applications such as sensing, which further broadens the application space of these waste-derived products.[16,17]

More recently, several research groups demonstrated the concept and route of converting polyolefin wastes to CO<sub>2</sub> capture carbon sorbents. [18–20] Particularly, PP mask-derived carbon fibers shows a good CO<sub>2</sub> sorption performance due to the presence of sulfur heteroatoms in the carbon framework, which is incorporated through sulfonation-induced crosslinking reactions. [21] However, routes for further functionalization of these mask-derived carbon fibers, such as activation and doping additional heteroatoms, are still underexplored. We note that while global usage dropped significantly with society returning to normalcy after the COVID-19, PP mask is still a common type of medical wastes which necessitates efficient upcycling methods. Herein, we report a simple method to produce high surface area, dual heteroatom-doped carbon fibers from PP-based masks. Specifically, sulfonation-based crosslinking is

employed, followed by direct carbonization with the presence of melamine which serves as a nitrogen doping source. Subsequently, chemical activation of carbons using KOH is performed, resulting in significantly enhanced surface area up to 1447  $\rm m^2/g$ . The resulting material after doping and activation exhibits excellent CO<sub>2</sub> capture performance, including high sorption capacity, selectivity, and stability. This work demonstrates the opportunity of further functionalizing PP mask-derived carbon materials for improving their environmental remediation performance, ultimately extending/enhancing their use and value through chemical upcycling.

# **Experimental section** *Materials*

PP-based surgical masks used in this study were acquired from CVS Health. We note that these surgical masks may contain additives and contaminates for promoting their functionality and processability. However, precisely understanding mask composition is not within the scope of this work. Indeed, this study focuses on developing a robust method to upcycling and functionalize mask waste, regardless of the presence of common additives. Fuming sulfuric acid (18–24% free SO<sub>3</sub> group) and melamine were purchased from Sigma Aldrich. Potassium hydroxide (KOH) was obtained from Fisher Scientific. Deionized (DI) water was obtained through a Milli-Q IQ 7003 ultrapure lab water purification system from Millipore Sigma.

# Sulfonation, doping, and carbonization of PP-derived mask samples

A surgical mask was first cut into small pieces and used as a model system representing fibril plastic waste. The non-woven outer layers were separated ( $\sim 0.63~g$  for each piece) and introduced into a 100 mL beaker containing approximately 40 mL of fuming sulfuric acid. A glass slide was placed on top of the mask pieces in order to ensure they were fully submerged throughout the crosslinking reaction. These mask pieces were then heated at 130 °C on a thermal plate for varied amount of time under stirring. After crosslinking, the reaction was cooled down to room temperature, and the masks were removed from the acid and washed with DI water for multiple times in order to remove all residual acids and/or other by-products. Crosslinked mask pieces were then fully dried under vacuum for at least 12 h.

Melamine was used as nitrogen dopant for preparing nitrogen, sulfur co-doped (or N, S-doped) carbon fibers. Specifically, sulfonated masks were mixed with melamine at a 1:1 mass ratio of mask to dopant, which were then carbonized in a tube furnace (MTI Corp., OTF-1200x) at 1°C/min up to 600°C, and then 5°C/ to 800°C under an  $\rm N_2$  atmosphere. The heating procedure was terminated after the temperature reached 800°C. After pyrolysis, doped carbons were washed three times by centrifuging them in DI water for 10 min. A control sample was also prepared by directly carbonizing sulfonated masks with the absence of melamine.

For the activation process, a 1:1 mass ratio of mask-derived, N, S-doped carbon to KOH was blended and then heated at 700°C for 1 h (temperature ramp: 5°C/min) in a N<sub>2</sub> atmosphere. Subsequently, the activated carbon was washed using DI water for at least five times for removing activation by-products and other un-reacted species. The sample was finally dried under vacuum for 12 h at 40°C.

# Characterization methods

In order to determine the chemical composition of masks before and after sulfonation, a PerkinElmer Frontier attenuated Fourier transform infrared (FTIR) spectrometer was used; 32 scans were obtained from a range of 4000-600 cm<sup>-1</sup>. Differential scanning calorimetry (DSC) was performed by Discover Series DSC 250 (TA Instruments) to characterize PP crystallinity degree of sulfonated masks with respect to time. The reference enthalpy of PP is 207 J/g. Thermogravimetric analysis (TGA) was employed for determining the carbon yield from crosslinked PP masks. Mass gain (from sulfonation reaction) was determined by comparing the mass of pristine masks to their sulfonated counterparts, and the carbon yield was calculated by comparing the initial mass of the mask pieces to the final mass of resulting carbon fibers. A Zeiss Ultra 60 fieldemission scanning electron microscope (SEM) was used to investigate the morphological changes of PP-derived masks after each processing step, including crosslinking, doping/ carbonization, and activation. ImageJ analysis software was used to analyze the diameters of the fibers within the images. This instrument was also used to perform energy dispersive X-ray (EDX) microscopy, in order to determine the elemental content of each type of carbon fiber-based product. Adsorption-desorption isotherms of mask-derived carbons were determined through the use of a Micromeritics Tristar II under N2 at 77 K. Surface area and pore size distribution can be determined through Brunauer-Emmett-Teller (BET) analysis and Barrett-Joyner-Halenda model, respectively. Specifically, BET surface area is calculated using 4 points in the relative pressure range from 0.2 to 0.3. A comprehensive description of this technique can be found in previous literature. [22] Additionally, CO<sub>2</sub> uptake performance of mask-derived functional carbons was determined using Micromeritics Tristar II at 25°C (from 0.01 to 1 bar). Selectivity values were calculated by first recording adsorption isotherms of CO<sub>2</sub> and N<sub>2</sub> at 25°C. The slopes of the adsorption isotherms at low pressures represent Henry's constant which describes the molecule-surface interactions between the adsorbate and the adsorbent. These values were extracted below 0.1 bar and used to determine selectivity by employing Eq. 1:

$$\alpha = \frac{K_{CO_2}}{K_{N_2}} \tag{1}$$

where  $\alpha$  is the selectivity,  $K_{CO_2}$  is Henry's constant for adsorption of  $CO_2$ , and  $K_{N_2}$  is Henry's constant for adsorption of  $N_2$ . It is worth noting that this method for determining selectivity



is only relevant at low pressures and low adsorption levels. For studying selectivity outside of this pressure range and adsorbate loading, methods such as the ideal adsorption solution theory (IAST) is recommended. [23,24]

### **Results and discussion**

Previous work demonstrated the use of PP-derived masks as the starting materials for preparing carbon fibers and their efficient use in several applications, such as water remediation, carbon capture, and energy storage. [21,25-27] Building on these progresses, this work further explores the opportunity of synthesizing high surface area and dual heteroatom-doped carbon fibers from mask precursors, while developing fundamental understandings about how pore textures and carbon framework chemistry impact their CO<sub>2</sub> sorption performance. Figure 1(a) illustrates our synthesis process, including three steps of crosslinking, simultaneous doping and carbonization, and activation. Specifically, fuming acid was employed as the crosslinking agent, enabling much faster reaction kinetics than concentrated sulfuric acid. Additionally, melamine was used as the doping source for introducing nitrogen heteroatoms into the PP-derived carbon fibers. Activation step in this work was similar to a previous report.[28]

Sulfonation-induced crosslinking of PP masks involves multiple steps and mechanisms, including installing sulfonic acid groups into polymer backbones, homolytic dissociations, and the formation of unsaturated bonds through olefination. [26] Subsequently, the alkene groups along functionalized PP backbones serve as cornerstones for further secondary additions, rearrangements, and eventual crosslinking. Figure 1(b) displays the progression of this reaction through understanding the increase in mass gain and the loss of crystallinity of PP-derived masks as a function of reaction time. It was found that crosslinking reaction of PP masks can be rapidly accomplished

within only 20 min, confirmed by their mass gain reaching a plateau value of ~55% as well as a complete loss of crystallinity (Figure S1). Notably, this reaction rate is much faster than other works using concentrated sulfuric acid as the crosslinking agent, due to the presence of free SO<sub>3</sub> groups in fuming acid that provides enhanced reactivity. The loss of PP crystallinity, upon sulfonation/crosslinking, is due to combined effects of installing sulfonic acid groups into polymer backbones and the crosslinked nature of PP, completely hindering chain mobility to re-crystallize. These observations were consistent with several previous reports associated with PP sulfonation. [26] To further confirm the successful crosslinking of PP using fuming acid, FTIR spectra were performed on untreated and sulfonated PP-derived masks (after 20 min crosslinking time) to study the changes in their chemical compositions. Specifically, the band at 2929 cm<sup>-1</sup> related to the C-H stretch in PP was completely diminished upon sulfonation. Similarly, a broad band corresponding to hydroxyl groups appeared at 3335 cm<sup>-1</sup>, which are associated with the sulfonic acid groups attached on PP backbone. Formation of double bonds for crosslinking is confirmed by the appearance of a band at 1603 cm<sup>-1</sup>, corresponding to alkene groups. Moreover, the enhanced reaction kinetics from using fuming acid does not disrupt the appearance of fibral structures of PP-derived masks after crosslinking, as shown in Fig. 1(d). Approximately 15% diameter shrinkage of PP fibers was observed from the sulfonation step, reducing from 20.3 µm to 16.8 µm (Figure S2), which can be attributed to the fiber densification upon crosslinking and is consistent with literature results.[26]

Figure 2(a) shows the TGA curve of crosslinked PP masks, indicating a 36 wt% carbon yield from sulfonated PP upon pyrolysis at 800°C under N<sub>2</sub> atmosphere. As a comparison, neat PP does not yield any carbon. For nitrogen doping, sulfonated PP fibers were first mixed with melamine, which is a common dopant, followed by simultaneous doping and carbonization.

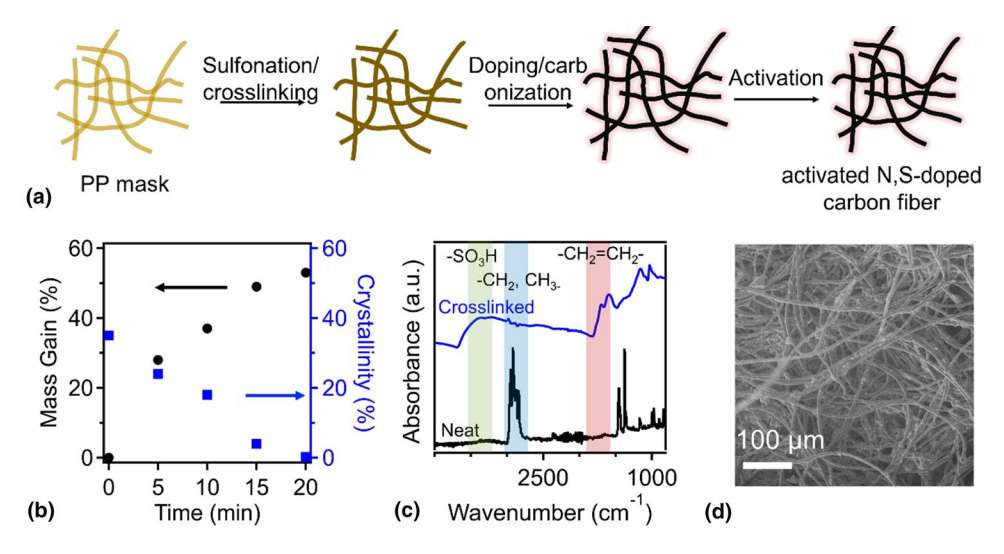
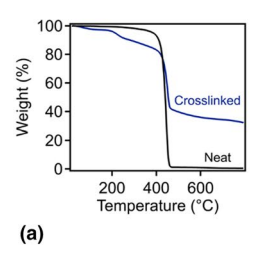
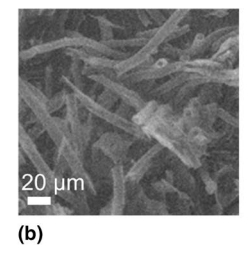
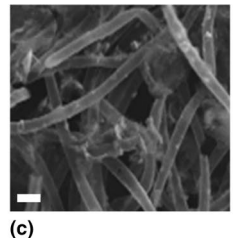


Figure 1. (a) Synthesis scheme of activated, N, S-doped carbon fibers from polypropylene (PP) masks. (b) Mass gain and crystallinity changes in sulfonated PP-derived mask as a function of reaction time. (c) FTIR spectra of untreated and crosslinked (sulfonated) mask pieces, demonstrating the changes in the chemical composition. (d) SEM image of crosslinked PP-derived mask (reaction time: 20 min).







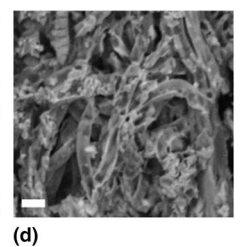
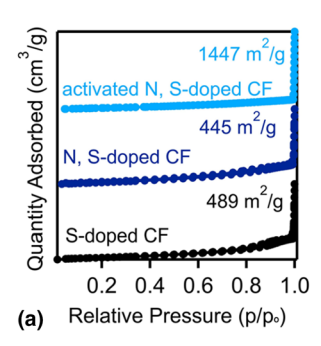


Figure 2. (A) TGA of neat and crosslinked PP fibers. SEM images of (b) carbon fibers from directly pyrolysis of crosslinked PP, (c) carbon fibers pyrolyzed with the presence of melamine, and (d) their morphology after a KOH activation step.



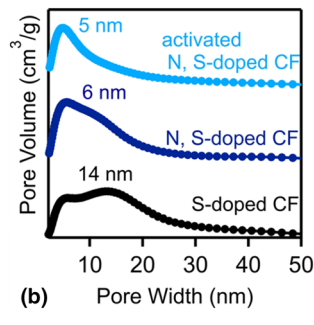


Figure 3. (a) Nitrogen adsorption-desorption isotherm of S-doped CF, N, S-doped CF, and activated N, S-doped CF at 77K, (b) and their derived pore size distributions. The averaged pore size of different CF products is labeled in the Figure.

Specifically, during this process, melamine can be decomposed to gaseous by-products, such as ammonia, to effectively incorporate nitrogen functional groups into carbon framework. [29,30] While the doping mechanism of these materials is not fully understood, it can be seen as analogous to doping graphene oxide with melamine.[31] Oxygen containing functionalities within the precursor facilitate different reactions such as hydrogen abstraction, dehydration, and deoxidation with species that are formed through the decomposition of the dopant. In turn, heteroatom containing functional groups are covalently bound to the precursor leading to their incorporation into the carbon framework. The presence of sulfur and nitrogen heteroatoms in carbon framework are known to enhance their affinity to capture CO2 molecules due to enhanced Lewis acid-base interactions.[32,33] Figure 2(b-c) shows the microstructure of carbon fibers from pyrolysis of crosslinked PP-masks with the absence and presence of melamine, respectively. Specifically, Fig. 2(b) shows that carbon fibers with an averaged diameter of 14.4 µm, which is ~15% lower than the crosslinked PP fibers. Reduced volume (or fiber diameter) upon conversion of polymer to carbon is anticipated due to a much higher density of carbon compared to sulfonated PP. For nitrogen-doped samples, their fiber diameters were found to be 14 µm, suggesting that doping reaction in this work does not significantly impact the fiber diameters of resulting carbons. Nevertheless, both carbonized masks show that the fibril structure can be successfully retained, while some disruptions in their uniformity were

observed. After KOH activation at 700°C for 1 h, structures of these co-doped carbon fibers became significantly more disordered, as shown in Fig. 2(d).

Many practical applications of porous carbon materials, such as dye sorption, CO2 uptake, and supercapacitors, are largely dependent on their pore textures, particularly associated with surface area. [34-36] Figure 3(a) shows the liquid nitrogen adsorption-desorption isotherms of different mask-derived carbon samples, including direct pyrolysis (no additional functionalization step) and after doping and activation treatments. These samples are referred as S-doped CF, N, S-doped CF, and activated N, S-doped CF, respectively. The surface area of S-doped CF, yielded from carbonization of sulfonated masks is approximately 489 m<sup>2</sup>/g, while the N, S-doped CF has a surface area of 445 m<sup>2</sup>/g. The reduced surface area of mask-derived carbons after doping is similar to many previous reports, which can be explained by the added mass from the inclusion of nitrogen heteroatoms into the carbon framework. Upon activation, these carbon products exhibit a significantly enhanced surface area, reaching up to 1447 m<sup>2</sup>/g, which indicates a more than two-fold increase compared to their analog prior to KOH treatment. Furthermore, pore size distributions of these carbons are shown in Fig. 3(b). S-doped CF exhibits a peak corresponding to an averaged pore width of 14 nm, which reduces to 6 nm after nitrogen doping and 5 nm after KOH activation; these two changes can be explained by the expansion of carbon framework after inclusion of heteroatoms and hightemperature activation leading to pore shrinkage, respectively. Furthermore, the incorporation of heteroatoms, including nitrogen, sulfur, and oxygen, in the carbon framework can alter the framework electronegativity, which are useful for enhancing the favorable interactions between carbon matrix and CO<sub>2</sub> guest molecules. As shown in Figures S3-S5 and Tables S1-S3, EDX data demonstrates the presence of heteroatoms in all iterations of the carbon fibers. S-doped CF has 89 wt% carbon, 8 wt% oxygen, and 3 wt% sulfur, which is consistent with our previous reports.<sup>[19]</sup> Our doping reaction introduces up to 22 wt% nitrogen into the carbon framework. For activated N, S-doped CF, 15 wt% nitrogen and 2 wt% sulfur were recorded. Slight reductions in nitrogen and sulfur content can be attributed to a second exposure to high temperatures in the activation step, causing loss of functional groups. Nevertheless, these results



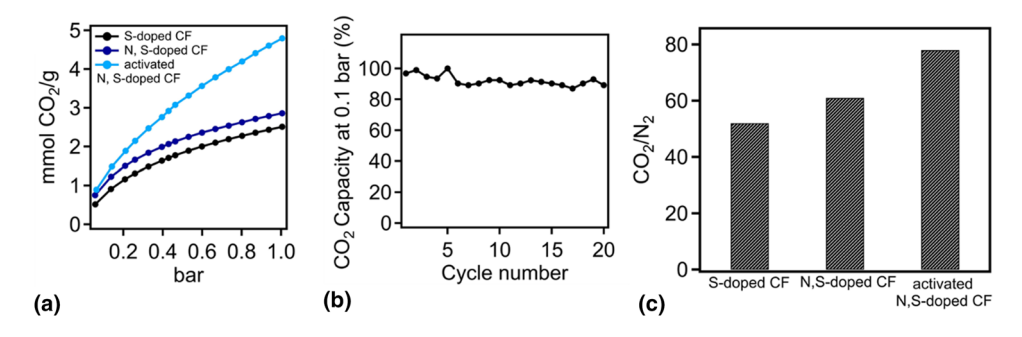


Figure 4. (a) CO<sub>2</sub> uptake capacity of different PP mask-derived carbon fiber sorbents, with improved performance upon nitrogen doping and KOH activation. (b) CO<sub>2</sub> sorption capacity of activated, N, S-doped CF at 0.1 bar and room temperature as a function of cycle number. (c) CO<sub>2</sub>/N<sub>2</sub> selectivity of different CFs as labeled in the Figure.

confirmed that heteroatoms in mask-derived CFs can still be mostly retained even after rigorous KOH activation reaction.

As previously discussed, this work focuses on upcycling and functionalization of PP-based mask wastes to CO<sub>2</sub> capture sorbents, enabling their value-enhanced use for addressing an urgent environmental challenge. While previous work reported the use of polyolefin waste as the feedstock to fabricate porous carbons, the opportunity of further functionalization was less explored. Herein, CO2 sorption capacity of different types of PP mask-derived carbon fibers were investigated, as shown in Fig. 4(a). S-doped CF exhibits the lowest sorption capacity at room temperature, which is 0.5 mmol/g at 0.1 bar and 2.4 mmol/g at 1 bar. Upon nitrogen doping and despite the slight reduction in the BET surface area, N, S-doped CF has an improved CO<sub>2</sub> uptake capacity of 0.8 mmol/g and 2.8 mmol/g at 0.1 bar and 1 bar, respectively. This increase in sorption performance can be attributed to the nitrogen functional groups in the carbon framework, which alter the polarity of the carbon surfaces and enhance their interactions with CO2 guest molecules. In a previous study, Xing and co-workers employed quantum chemical calculations and FT-IR measurements to elucidate that the presence of nitrogen heteroatoms in carbon framework facilitates the formation of hydrogen-bonding interactions between the carbon and CO2, providing an important mechanism for improving CO<sub>2</sub> sorption performance. [37] After activation, these high surface and dual heteroatom-doped porous carbon fibers (i.e., activated, N, S-doped CF) can exhibit excellent CO<sub>2</sub> sorption capacity at room temperature, which is 0.9 mmol/g at 0.1 bar and 4.8 mmol/g at 1 bar, surpassing most previous work of using plastic waste to manufacture carbon capture sorbents. We attribute this high performance to the presence of nitrogen and sulfur heteroatoms in the carbon framework, as well as the high surface area obtained through chemical activation. Figure 4(b) shows the stability of CO<sub>2</sub> sorption capacity of activated and N, S-doped CF at 0.1 bar; this condition of CO<sub>2</sub> concentration) is similar to common flue gas systems in chemical plants. It was found these materials show less than 10% CO<sub>2</sub> capacity loss after 20 sorption cycles, and less than 2% loss was observed after the fifth cycle. To further evaluate the potential of these PP mask-derived porous

CF sorbents to address practical applications, we investigate their gas selectivity of CO<sub>2</sub> against N<sub>2</sub>. Figure 4(c) showcases that nitrogen doping and activation can lead to improved selectivity from 52 (S-doped CF) to 61 and 78 for N, S-doped CF, and activated sample, respectively. These results are higher to others found in literature, [38,39] which can be attributed to the combined effects of heteroatom doping leading to more favorable interactions between carbon and CO<sub>2</sub> molecules, as well as the improved pore textural properties upon activation; note that previous studies indicate that reacting carbon with KOH at 700°C can generate excess amount of interconnected and continuous micropore channels. Additionally, a recent work demonstrated that similar nitrogen and sulfur doped corn starch-derived porous carbons exhibit slightly higher selectivities ranging from 89 to 121, which is likely due to increased surface area compared to the mask-derived carbon. [33] Overall, these results suggest that the use of PP-based mask waste as feedstock, in conjunction with simple and scalable methods for carbonization and functionalization, can yield high performance CO2 capture sorbents for collectively addressing the challenges in plastic waste recycling and greenhouse gas remediation.

# **Conclusion**

This study demonstrates the upcycling of PP-derived surgical masks to activated, N, S-doped carbon fibers, which can exhibit excellent performance for CO<sub>2</sub> uptake, including high capacity, selectivity, and stability. Particularly, the use of fuming sulfuric acid leads to fast crosslinking kinetics of PP, while steps of doping and activation can further enhance the functionality of PP mask-derived carbon fibers, including a high surface area up to 1447 m²/g and high heteroatom content of both sulfur (2 wt%) and nitrogen functional groups (15 wt%). These advantageous features endow strong and favorable interactions between porous carbon surfaces and CO<sub>2</sub> guest molecules. As a result, activated N, S-doped carbon fibers can exhibit a high CO<sub>2</sub> adsorption capacity of 4.8 mmol/g at room temperature and 1 bar, as well as a high CO<sub>2</sub>/N<sub>2</sub> selectivity reaching up to 78, making them potential viable options for addressing flue

gas emissions. Overall, this work advances the use of mask wastes through enabling their high performance for addressing emerging environmental threats.

# **Acknowledgments**

The authors thank partial support from Mississippi SMART Business Act, National Science Foundation (CMMI-2239408) and the University of Southern Mississippi for generous financial support.

#### **Author contributions**

AGO and ZQ were responsible for experiment design during this project. Majority of the experiments were carried out by AGO, with assistance from MR and PS This manuscript was primarily written by AGO and ZQ, while all authors contributed. ZQ supervised all work through this project.

# **Funding**

University of Southern Mississippi, Division of Civil, Mechanical and Manufacturing Innovation, 2239408, Zhe Qiang.

# **Data availability**

Data of this work are available from the corresponding author based upon reasonable request.

### **Declarations**

#### Conflict of interest

The authors declare there is no conflict of interest.

#### Supplementary Information

The online version contains supplementary material available at https://doi.org/10.1557/s43579-023-00419-1.

#### References

- C. Mora, D. Spirandelli, E.C. Franklin, J. Lynham, M.B. Kantar, W. Miles, C.Z. Smith, K. Freel, J. Moy, L.V. Louis, E.W. Barba, K. Bettinger, A.G. Frazier, J.F. Colburn IX. N. Hanasaki, E. Hawkins, Y. Hirabayashi, W. Knorr, C.M. Little, K. Emanuel, J. Sheffield, J.A. Patz, C.L. Hunter, Nat. Clim. Change 8, 1062-1071 (2018). https://doi.org/10.1038/s41558-018-0315-6
- K. Lyu, X. Zhang, J.A. Church, A.B.A. Slangen, J. Hu, Nat. Clim. Change 4, 1006-1010 (2014). https://doi.org/10.1038/nclimate2397
- L. Estevez, D. Barpaga, J. Zheng, S. Sabale, R.L. Patel, J.G. Zhang, B.P. McGrail, R.K. Motkuri, Ind. Eng. Chem. Res. 57, 1262-1268 (2018). https://doi.org/10.1021/acs.iecr.7b03879
- C. Chen, H. Huang, Y. Yu, J. Shi, C. He, R. Albilali, H. Pan, Chem. Eng. J. 353, 584-594 (2018). https://doi.org/10.1016/j.cej.2018.07.161
- C. Chen, D.W. Park, W.S. Ahn, Appl. Surf. Sci. 283, 699-704 (2013). https:// doi.org/10.1016/j.apsusc.2013.07.005
- L. Yagoob, T. Noor, N. Igbal, ACS Omega 7, 13403-13435 (2022). https://doi. org/10.1021/acsomega.1c07291
- J. Choi, I. Yang, S.S. Kim, S.Y. Cho, S. Lee, Macromol Rapid Commun (2022). https://doi.org/10.1002/MARC.202100467

- 8. K.M. Wyss, D.X. Luong, J.M. Tour, Adv. Mater. 34, 2106970 (2022). https:// doi.org/10.1002/adma.202106970
- W. Chen, C. Ge, J.T. Li, J.L. Beckham, Z. Yuan, K.M. Wyss, P.A. Advincula, L. Eddy, C. Kittrell, J. Chen, D.X. Luong, R.A. Carter, J.M. Tour, ACS Nano 16, 6646-6656 (2022). https://doi.org/10.1021/acsnano.2c01136
- 10. A. Fivga, I. Dimitriou, Energy 149, 865-874 (2018). https://doi.org/10. 1016/j.energy.2018.02.094
- 11. Y. Zhang, D. Duan, H. Lei, E. Villota, R. Ruan, Appl. Energy 251, 113337 (2019). https://doi.org/10.1016/j.apenergy.2019.113337
- 12. J.M. Younker, T. Saito, M.A. Hunt, A.K. Naskar, A. Beste, J. Am. Chem. Soc. 135, 6130-6141 (2013). https://doi.org/10.1021/ja3121845
- 13. M.A. Hunt, T. Saito, R.H. Brown, A.S. Kumbhar, A.K. Naskar, Adv. Mater. 24, 2386-2389 (2012). https://doi.org/10.1002/adma.201104551
- 14. S. Villagómez-Salas, P. Manikandan, S.F. Acuña Guzmán, V.G. Pol, ACS Omega 3, 17520-17527 (2018). https://doi.org/10.1021/acsomega. 8b02290
- 15. Y. Lian, M. Ni, Z. Huang, R. Chen, L. Zhou, W. Utetiwabo, W. Yang, Chem. Eng. J. 366, 313-320 (2019). https://doi.org/10.1016/j.cej.2019.02.063
- 16. Y. Wang, R. Singh, S. Chaudhary, B. Zhang, S. Kumar, IEEE Trans. Instrum. Meas. 71, 9504609 (2022). https://doi.org/10.1109/TIM.2022.3160536
- 17. G. Li, Q. Xu, R. Singh, W. Zhang, C. Marques, Y. Xie, B. Zhang, S. Kumar, IEEE Sens. J. 22, 16904-16911 (2022). https://doi.org/10.1109/JSEN.
- 18. A. Abbasi, M.M. Nasef, S. Kheawhom, R. Faridi-Majidi, M. Takeshi, E. Abouzari-Lotf, T. Choong, Radiat. Phys. Chem. 156, 58-66 (2019). https:// doi.org/10.1016/j.radphyschem.2018.10.015
- 19. R. Wang, H.Y. Zhang, P.H.M. Feron, D.T. Liang, Sep. Purif. Technol. 46, 33-40 (2005). https://doi.org/10.1016/j.seppur.2005.04.007
- 20. W.A. Algozeeb, P.E. Savas, Z. Yuan, Z. Wang, C. Kittrell, J.N. Hall, W. Chen, P. Bollini, J.M. Tour, ACS Nano 16, 7284-7290 (2022). https://doi.org/10. 1021/acsnano.2c00955
- 21. M. Robertson, A.G. Obando, B. Nunez, H. Chen, Z. Qiang, ACS Appl. Eng. Mater. 1, 165-174 (2022). https://doi.org/10.1021/ACSAENM.2C00030
- 22. M. Naderi, Prog. Filtr. Sep. (2015). https://doi.org/10.1016/B978-0-12-384746-1.00014-8
- 23. M. Oschatz, M. Antonietti, Energy Environ. Sci. 11, 57-70 (2018). https:// doi.org/10.1039/C7EE02110K
- 24. Y.S. Bae, R.Q. Snurr, Angew. Chem. Int. Ed. 50, 11586-11596 (2011). https://doi.org/10.1002/ANIE.201101891
- 25. X. Hu, Z. Lin, Ionics 27, 2169-2179 (2021). https://doi.org/10.1007/ s11581-021-03949-7
- 26. G. Lee, M. Eui Lee, S.S. Kim, H.I. Joh, S. Lee, Ind. Eng. Chem. 105, 268-277 (2022). https://doi.org/10.1016/j.jiec.2021.09.026
- 27. W. Yang, L. Cao, W. Li, X. Du, Z. Lin, P. Zhang, Ionics 28, 3489-3500 (2022). https://doi.org/10.1007/s11581-022-04567-7
- J. Wang, S. Chen, J.Y. Xu, L.C. Liu, J.C. Zhou, J.J. Cai, New Carbon Mater. 36, 1081-1090 (2021). https://doi.org/10.1016/S1872-5805(21)60074-4
- 29. Z. Qiang, Y. Xia, X. Xia, B.D. Vogt, Chem. Mater. 29, 10178–10186 (2017). https://doi.org/10.1021/acs.chemmater.7b04061
- 30. Z. Qiang, Y.M. Chen, Y. Xia, W. Liang, Y. Zhu, B.D. Vogt, Nano Energy 32, 59-66 (2017). https://doi.org/10.1016/J.NANOEN.2016.12.018
- 31. Z.H. Sheng, L. Shao, J.J. Chen, W.J. Bao, F. Bin Wang, X.H. Xia, ACS Nano 5, 4350-4358 (2011). https://doi.org/10.1021/NN103584T
- 32. W. Tian, H. Zhang, H. Sun, A. Suvorova, M. Saunders, M. Tade, S. Wang, Adv. Funct. Mater. 26, 8651-8661 (2016). https://doi.org/10.1002/adfm. 201603937
- 33. G. Nazir, A. Rehman, S.J. Park, J. CO2 Util. 51, 101641 (2021). https:// doi.org/10.1016/j.jcou.2021.101641
- 34. H.L. Parker, A.J. Hunt, V.L. Budarin, P.S. Shuttleworth, K.L. Miller, J.H. Clark, RSC Adv. 2, 8992-8997 (2012). https://doi.org/10.1039/C2RA2
- Y. Lv, F. Zhang, Y. Dou, Y. Zhai, J. Wang, H. Liu, Y. Xia, B. Tu, D. Zhao, J. Mater. Chem. 22, 93-99 (2011). https://doi.org/10.1039/C1JM12742J
- Z. Zhang, J. Zhou, W. Xing, Q. Xue, Z. Yan, S. Zhuo, S.Z. Qiao, Phys. Chem. Chem. Phys. 15, 2523-2529 (2013). https://doi.org/10.1039/C2CP4 4436D
- 37. W. Xing, C. Liu, Z. Zhou, L. Zhang, J. Zhou, S. Zhuo, Z. Yan, H. Gao, G. Wang, S.Z. Qiao, Energy Environ. Sci. 5, 7323-7327 (2012). https://doi. org/10.1039/C2EE21653A



- 38. H. Cong, M. Zhang, Y. Chen, K. Chen, Y. Hao, Y. Zhao, L. Feng, Carbon 92, 297-304 (2015). https://doi.org/10.1016/j.carbon.2015.04.052
- 39. Y. Zhao, L. Zhao, K.X. Yao, Y. Yang, Q. Zhang, Y. Han, J. Mater. Chem. 22, 19726-19731 (2012). https://doi.org/10.1039/C2JM33091A

Publisher's Note Springer Nature remains neutral with regard to jurisdictional claims in published maps and institutional affiliations.

Springer Nature or its licensor (e.g. a society or other partner) holds exclusive rights to this article under a publishing agreement with the author(s) or other rightsholder(s); author self-archiving of the accepted manuscript version of this article is solely governed by the terms of such publishing agreement and applicable law.